Near edge structure of X-ray absorption in the CCD response

G. Prigozhin (MIT), J. Woo (SAO),
M. Bautz, G. Ricker (MIT), J. Gregory (Lincoln Lab), B. Harris (SAO),
E. Gullikson (ALS), S. Kraft, and G. Ulm (PTB, BESSY)

1 Introduction

In order to produce an accurate model of CCD quantum efficiency it is very important to know precisely the optical constants of the materials comprising the gate structure of the device. Widely used Henke data are quite inaccurate at energies close to the absorption edges. We undertook an effort to measure the transmission of the corresponding films in order to to fill in this gap.

The CCD gate structure contains three different materials: silicon dioxide, silicon nitride (Si_3N_4), and polycrystalline silicon, which is heavily doped with phosphorus. All the X-ray absorption edges of these materials, namely, silicon L (100 eV), nitrogen K (400 eV), oxygen K (532 eV), and silicon K (1840 eV) are within the range of interest for ACIS.

In the course of technology development for manufacturing backside CCD, Lincoln Lab implemented a technique for etching away the thick silicon substrate, leaving only a thin layer of material at the surface of the wafer. This technology turned out to be exceptionally well suited for making thin films supported by a rigid frame, allowing them to be handled easily. Usually, at low energies the transmission of a material is derived from the results of the measurement of total electron yield. With the Lincoln Lab technology it is possible to make extremely thin free standing films and measure transmission directly. We used synchrotron radiation to measure the transmission of these materials as a function of energy. There is no single beamline which can cover such a wide range of energies, and for this reason measurements were performed at three different synchrotrons.

2 Sample preparation

All the samples were prepared in a similar manner. A film was grown on the silicon substrate and then silicon from the back side of the wafer was etched away in a circular opening approximately 0.5 centimeter in diameter. The etching stops when the film is reached. This results in an extremely thin film sitting on the top of the silicon frame. The cross section of such structure is shown in Fig. 1.

The following samples were prepared at Lincoln Lab for the transmission measurements:
1. Thin SiO_2 film (dry oxidation of Si wafer at 1000^o C, a process identical to the one used for CCD gate oxide growth), nominally 0.14 microns thick.
2. Thick SiO_2 film (wet oxidation at 1000^o C, a process used for channel stop oxide growth), approximately 1.5 microns thick.
3. A sandwich of $SiO_2 + Si_3N_4 + SiO_2$, a copy of the CCD gate insulator structure, nominal

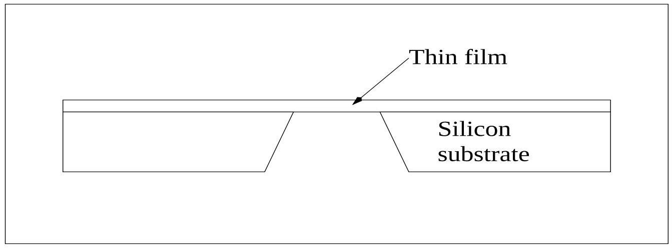

Figure 1: Cross section of the thin film sample.

thicknesses 0.06 + 0.03 + 0.015 microns.
4. Phosphorus doped polycrystalline silicon, 0.6 microns thick.
5. The same polycrystalline silicon film partially oxidized, nominally 0.46 + 0.2 microns of Si+SiO_2 respectively.

3 Measurement details

X-ray transmission measurements of samples 1 and 3 at low energies (60 eV – 900 eV) were performed at the Advanced Light Source (Lawrence Berkeley National Lab), beamline number 6.2.3, which is equipped with a grating monochromator with superb energy resolution (resolving power 7000). Three different gratings are needed to cover the entire energy range. For each grating the interval is further divided into two or three subranges due to the necessity of using different filters to suppress higher orders. For this reason a dataset for each sample consists of 8 separate subsets. It should be noted that changing of the grating requires realignment of the beam.

Only samples 1 and 3 were characterized at ALS. Three other samples were too thick for the measurement in this energy range, being opaque at energies below 300 – 400 eV and above the O K edge (SiO_2 sample). The energy step in the region from 360 to 580 eV containing nitrogen and oxygen edges was set to 0.25 eV, to 0.5 eV for energies below 180 eV (around the Si L edge), and 1 eV for the rest of the energy range.

Transmission at energies around the silicon K edge was measured at two other synchrotrons: at BESSY (Berlin) and at the Synchrotron Radiation Center (Madison, Wisconsin). The Canadian Double Crystal Beamline at the SRC has a double crystal monochromator with a resolution of 0.9 eV. It utilizes a pair of InSb(111) crystals (instead of the more commonly used in this range silicon), which is important for this measurement in order to avoid silicon edge "steps" in the incoming flux. Due to the low energy of electrons in the storage ring (800 MeV) and the double crystal arrangement of the monochromator, this beamline has very low higher order light penetration (below 0.2%). The data were taken in the range from 1770 to 2500 eV. The energy step was 0.25 eV around Si edge (from 1830 to 1860 eV), and 1 eV for the rest of the range. The accuracy and reproduceability of the SRC data is better than 0.1%, the noise being hardly noticeable.

At BESSY measurement were made over a wider range, from 1300 eV to 3000 eV. In general BESSY results are much noisier, but they are very valuable since they span a wider range and this helps to constrain the thickness of the films more reliably.

Since the X-ray flux emitted by a storage ring is continuously changing, it is necessary to normalize the output intensity to the input flux. This requires two detectors for any measurement - one in front, and one behind the sample. A solid state X-ray detector was installed downstream from the sample to register the output flux. At all three beamlines it was an uncovered Hamamatsu GaAsP photodiode G1127-02. Again, this was one of the precautions taken to avoid silicon absorption edges anywhere in the measurement system. Upstream from the sample a transparent beam normalization detector monitored the input flux. At ALS and BESSY this was a metal mesh whose electron yield was measured. At SRC a gas ionization chamber served as the beam normalization detector.

Each measurement consisted of two passes through the energy range – one with the sample in the beam, another one with the sample out. The ratio of the two normalized fluxes is the transmission of the film.

4 Measurement results.

a. Silicon L, nitrogen and oxygen K edges

In Fig. 2 the solid line shows the transmission of the thin SiO_2 film at energies below 800

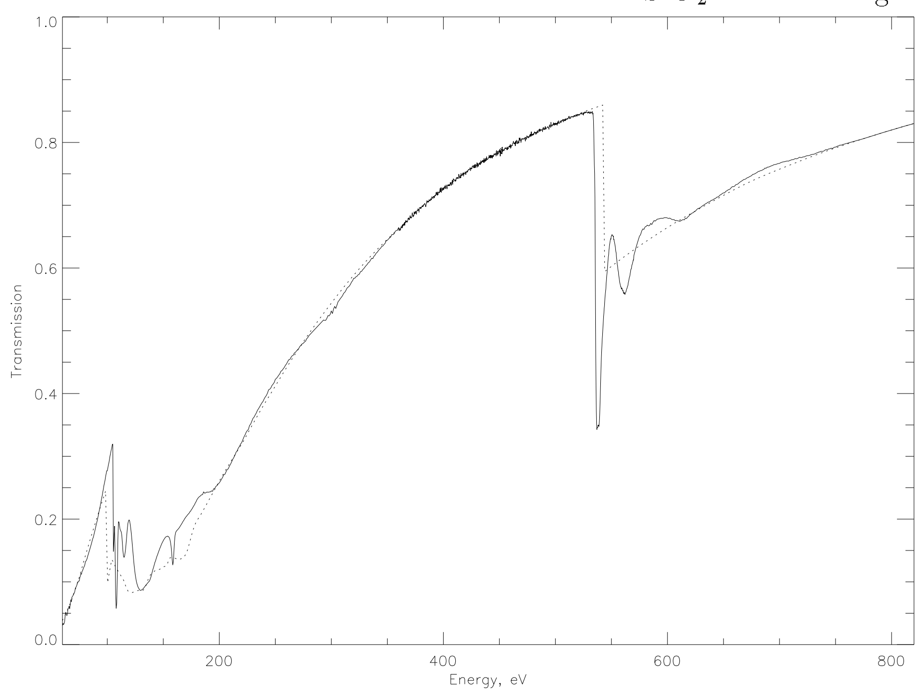

Figure 2: Transmission of the thin SiO_2 film as a function of energy (solid line). Dotted line represents standard Henke data.

eV. Very strong near-edge oscillations can be seen at energies above the silicon L and oxygen K absorption edges. In the areas where near-edge structure does not play a significant role, a fit to the standard Henke data was made with a thickness of the film as a free parameter. The best fit thickness was found to be 0.157 microns, and the corresponding transmission curve is shown on Fig. 2 as a dotted line. The deviation of the measured transmission from the Henke data is very strong above the absorption edges, and the edges themselves are shifted. The structure above 100 eV corresponds to silicon L_1, L_2, and L_3 edges at 158, 107, and 105 eV respectively. At the oxygen edge a very strong resonant absorption peak is found at 538 eV.

A transmission curve for the $SiO_2 + Si_3N_4 + SiO_2$ sandwich (which is an exact copy of the CCD gate isolator) is shown on the Fig. 3. In addition to the silicon and oxygen edges this plot shows a prominent nitrogen K edge, also shifted from the tabulated atomic value. The transmission of this sandwich was modeled as a combination of the Henke-derived Si_3N_4 transmission and the experimentally measured transmission of SiO_2. The best fit (thicknesses of both materials being free parameters) is shown in Fig. 3 as the dotted line.

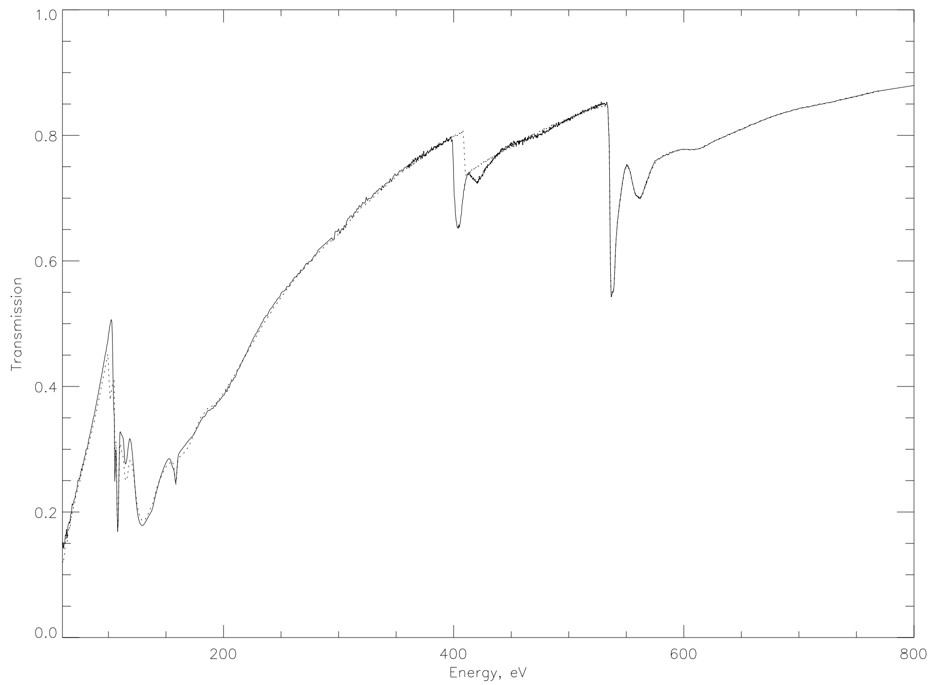

Figure 3: Transmission of the sandwich (solid line).

b. Silicon K edge

Fig. 4 contains absorption curves (not transmission!) of polysilicon, SiO_2, and the $SiO_2 + Si_3N_4 + SiO_2$ sandwich in the close vicinity of the silicon K edge. Each sample shows a sharp resonant peak right above the edge. Due to chemical shifts each of the three materials exhibits the silicon K-edge at slightly different energy. For polysilicon the peak is at 1841 eV; for SiO_2 it is at 1847.3 eV. The $SiO_2 - Si_3N_4 - SiO_2$ sandwich shows two distinct peaks which, although are not well-resolved, can be determined to be at 1847.3 and 1844.7 eV. The first one can obviously be attributed to SiO_2, while the second one originates from Si_3N_4. Polysilicon absorption shows a lot of structure due to its crystalline and ordered nature, whereas silicon dioxide has fewer peaks because it is amorphous and uncorrelated interference from remote atoms smears out the features.

The difference between the edge and resonant peak energies of polysilicon and SiO_2 can be seen very nicely in the oxidized polysilicon sample transmission in Fig. 5. A dashed line in this plot represents the result of fitting to this data the product of the transmissions of the separate films of polysilicon and SiO_2. The quality of the fit is so good that the dashed line can hardly be seen under the solid line.

In order to fill a gap in the data (no measurements were made in the range from 900 to 1300 eV), and also to extend the results to higher energies, we used Henke data (which should be adequate at energies far enough from the edges).

For each of the materials standard Henke data were used to fit the transmission at energies below the edge and far above the edge, where the near edge oscillations become weak. This procedure allows us to define the thickness of each film. The results are slightly different from the nominal values and are reflected in the labels in the above Figures. The densities of the materials used for those calculations were 2.19, 2.33 and 3.44 g/cm^3 for SiO_2, polysilicon and Si_3N_4, respectively. For both polysilicon and SiO_2 near-edge measurements were combined with Henke atomic scattering factors for silicon and oxygen, and mass absorption coefficient were produced in the range from 60 eV to 15 keV.

We encountered some difficulties in our attempt to separate optical constants of the Si_3N_4 film from the other components of the sandwich, most likely due to deviations from stoichiometry in one or more constituent layers. Because of that, for further applications we used a transmission of the sandwich as a whole unit, instead of deriving a mass absorption coefficient for each component.

5 CCD quantum efficiency.

Having all the absorption coefficients in hand it is possible to calculate the quantum efficiency of the CCD taking into account transmission of all the layers in the gate structure of the frontside CCD. In this model we accounted for the overlaps between the gates of the CCD, and assumed triangular edges of the channel stop oxide layer (which is a good approximation for the so-called "bird's beak" shape of those edges). Thicknesses of the layers were taken from the results of Scanning Electron Microscope (SEM) measurement of a sibling device cross section. In Fig. 6 is shown a plot of quantum efficiency as a function of energy for the frontside illuminated device. The dashed line in the Figure represents results of the quantum efficiency measurement of the frontside CCD at the SX700 beamline at BESSY. No fitting of the model to the data has been made for this plot. The deviation of the experimental points from the model at higher energies can be explained by the known second order light penetration of the SX700 monochromator at higher energies. In the analysis of the SX700 results the second order light counts are excluded in the CCD, while the reference photodiode cannot discriminate between orders. This results in the underestimation of the QE values for the CCD. It should also be mentioned that the above model accounts only for the transmission losses in all the layers (in great detail, though) and does not deal with the redistribution of counts into the low energy tail. This should not be a very significant factor for the frontside illuminated CCDs.

A similar plot for the backside illuminated device is shown in Fig. 7. Triangular points show the results of experimental measurements of the quantum efficiency of the backside illuminated device at the SX700 beamline at BESSY. The plot extends to very low energies around the silicon L edges, although the device loses its ability for spectral resolution below 250 eV. It still can be used for imaging, and its QE can be high enough, as can be seen from the Figure. The best agreement of experimental data with the transmission model was reached assuming a surface thickness of oxide layer of 0.055 microns, whereas the nominal thickness specified by Lincoln Lab is 0.035 microns. Besides that, we had to multiply the calculated QE by a factor of 0.96 to obtain an agreement with the experiment. This is expected, since for the backside devices a noticeable fraction of events is lost to the low energy tail. A more sophisticated model is necessary to account for this effect. As in the case with the frontside devices, a discrepancy at higher energies is attributed to second order light contamination.

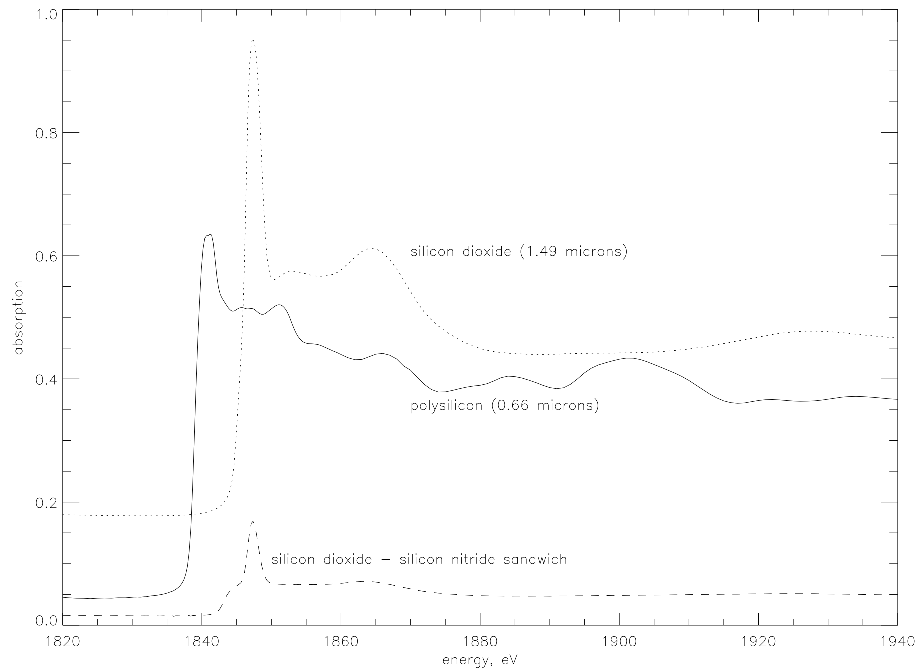

Figure 4: Absorption of the thin films of polysilicon (solid line), silicon dioxide (dotted line), and $SiO_2 - Si_3N_4$ (dashed line) sandwich.

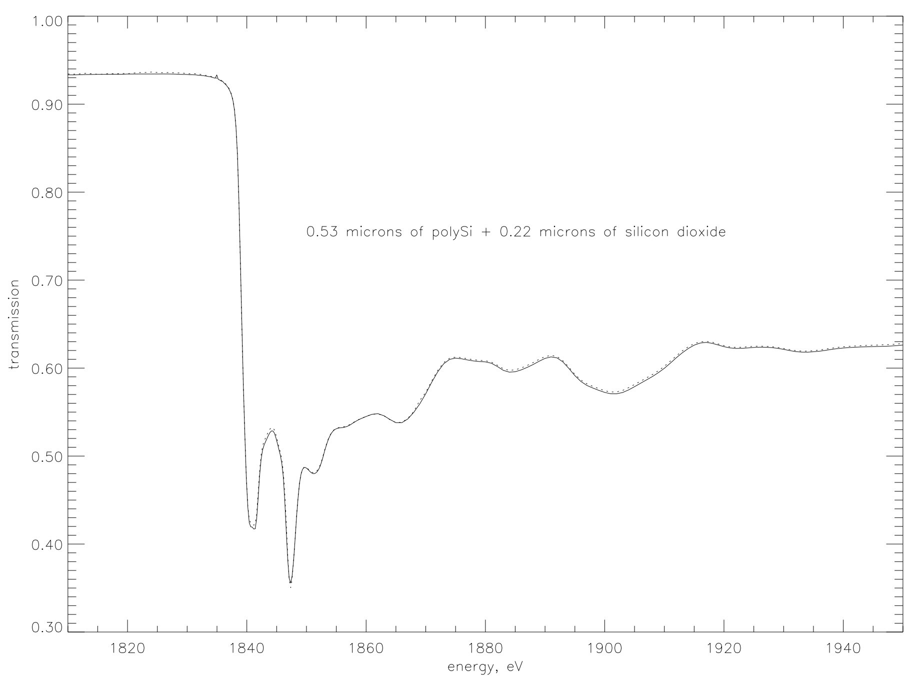

Figure 5: Transmission of the oxidized polysilicon film (solid line) and result of the best fit to it of the product of the polysilicon and SiO_2 transmissions (dotted line).

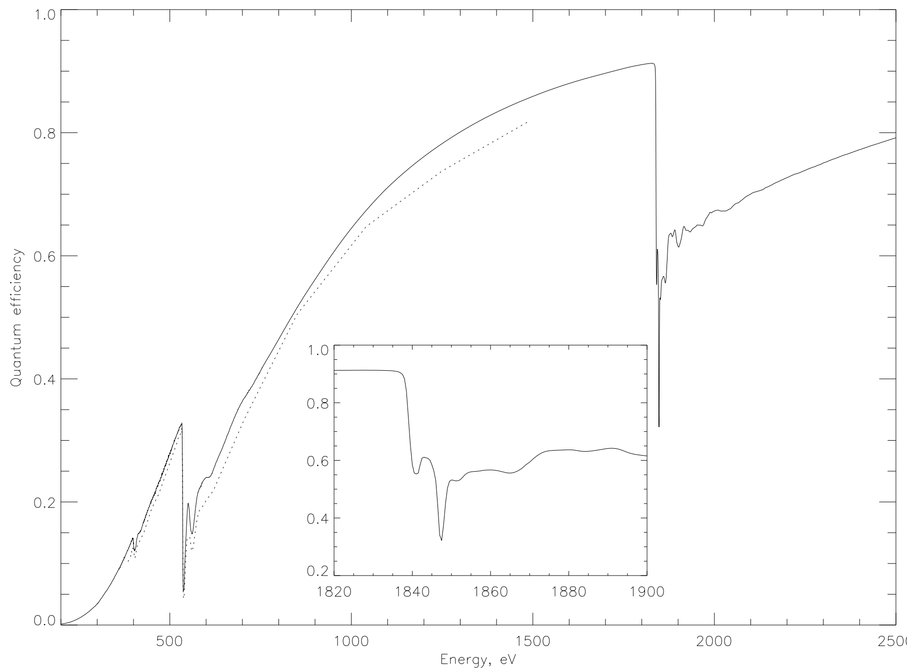

Figure 6: Quantum efficiency of the frontside illuminated CCD. Dashed line is the result of the QE measurement at SX700 line at BESSY.

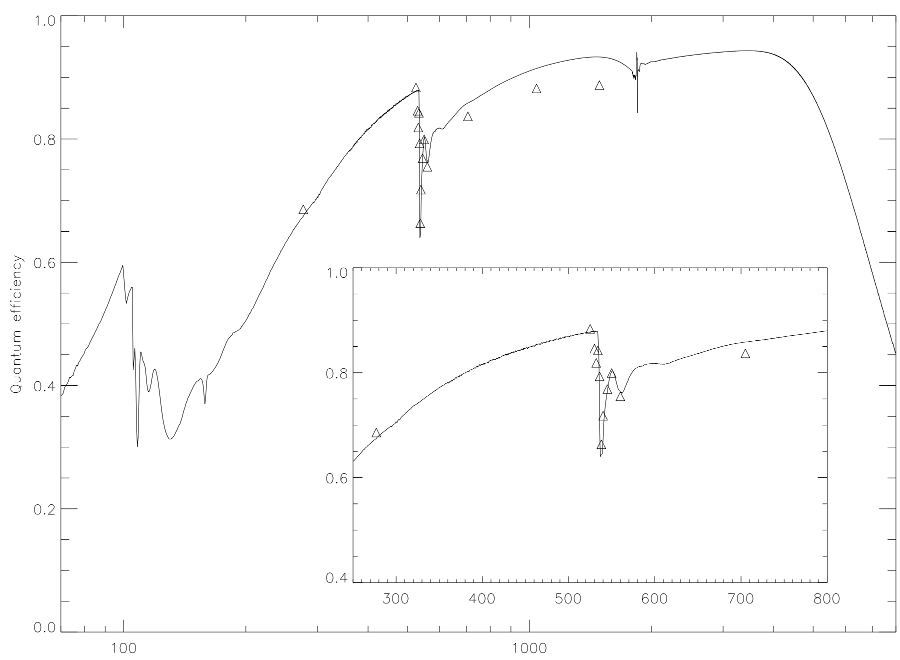

Figure 7: Quantum efficiency of the backside illuminated CCD. Triangles mark experimental results from SX700 at BESSY.